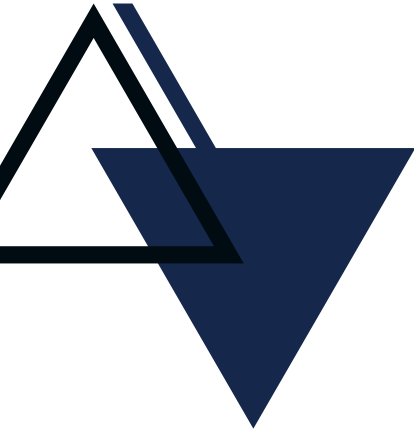


CHARACTERIZATION OF GEOMAGNETIC PULSATIONS in Corroboration with Solar wind Parameters

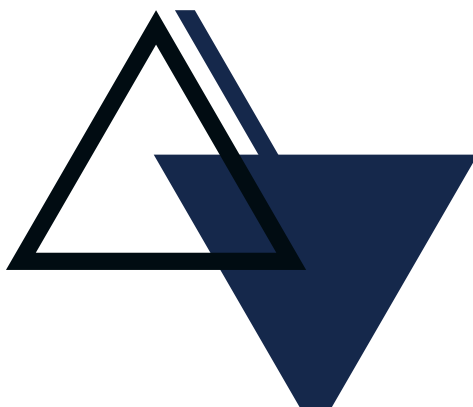
Presented by: Amal Ali Marzooq
Supervisor: Prof Ashwini Kumar

PHYCS499 | Department of Physics





- Introduction
- Aim of Research
- Methodology
- Results and Discussion
- Conclusion
- Future Work

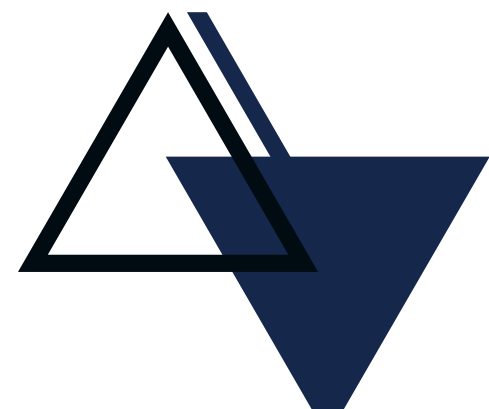




● Introduction



- A plasma consists of charged particles influenced by applied electric and magnetic fields and induces electric and magnetic fields in return.
- Hence the behavior of plasma is complex and models such as the magnetohydrodynamic (MHD) model are applied for simplicity.





● Introduction

The MHD model assumptions:

- The plasma is considered as a fluid under the adiabatic conditions.
- Magnetic induction dominates magnetic diffusion (large Raynold's number).
- The plasma fluid is tied to the magnetic field (frozen-in-plasma).





● Introduction

Using the MHD equations:

- The continuity equation: $\frac{\partial \rho_m}{\partial t} + \vec{\nabla} \cdot (\rho_m \vec{V}) = 0,$
- The equation of state: $\frac{d}{dt} \left(\frac{\vec{P}}{\rho_m^\gamma} \right) = 0 \rightarrow \vec{P} = C \rho_m^\gamma,$
- The momentum equation: $\rho_m \left(\frac{\partial \vec{V}}{\partial t} + (\vec{V} \cdot \vec{\nabla}) \vec{V} \right) = \vec{J} \times \vec{B} - \vec{\nabla} \vec{P},$
- Faraday's law: $\vec{\nabla} \times \vec{E} = -\frac{\partial \vec{B}}{\partial t},$
- Ampere's law: $\vec{\nabla} \times \vec{B} = \mu_0 \vec{J},$
- Ohm's law: $\vec{E} + \vec{V} \times \vec{B} = \eta \vec{J},$



● Introduction

The MHD general wave equation becomes:

$$\frac{\partial^2 \vec{v}}{\partial t^2} - v_s^2 \vec{\nabla}(\vec{\nabla} \cdot \vec{v}) + v_A \times (\vec{\nabla} \times \vec{\nabla} \times \vec{v} \times v_A) = 0$$

where $v_A = \vec{B}_0 / \sqrt{\mu_0 \rho_0}$ is the Alfven velocity, and $v_s = \sqrt{(\gamma \vec{P} / \rho_m)}$ is the speed of sound.

Assuming a planar velocity variation $\sim e^{i(\vec{k} \cdot \vec{r} - \omega t)}$ the ideal MHD dispersion equation is:

$$-\omega^2 \vec{v} + \vec{k}(\vec{k} \cdot \vec{v})(v_s^2 + v_A^2) - (\vec{k} \cdot v_A) \left[\vec{k}(v_A \cdot \vec{v}) - \vec{v}(\vec{k} \cdot v_A) + v_A(\vec{k} \cdot \vec{v}) \right] = 0$$



● Introduction

The different MHD wave modes:

Parallel to B_0 propagation

- When: $\vec{v} || \vec{B}_0 || \vec{k} \longrightarrow \boxed{\frac{\omega}{k_{||}} = v_s}$

which is a sound wave mode.

- When: $\vec{v} \perp \vec{B}_0 || \vec{k} \longrightarrow \boxed{\frac{\omega}{k_{||}} = v_A}$

which is the shear Alfvén mode.

Perpendicular to B_0 propagation

- When: $\vec{v} || \vec{k} \perp \vec{B}_0 \longrightarrow \boxed{\frac{\omega}{k_{\perp}} = \sqrt{v_s^2 + v_A^2}}$

which is a compressional wave mode.



● Introduction



Field Line Oscillations and String Analogy

The wave equation for the disturbances of the musical cord:

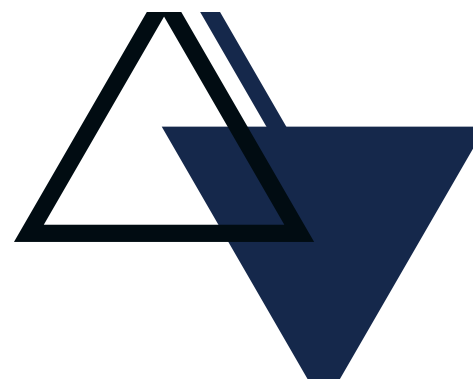
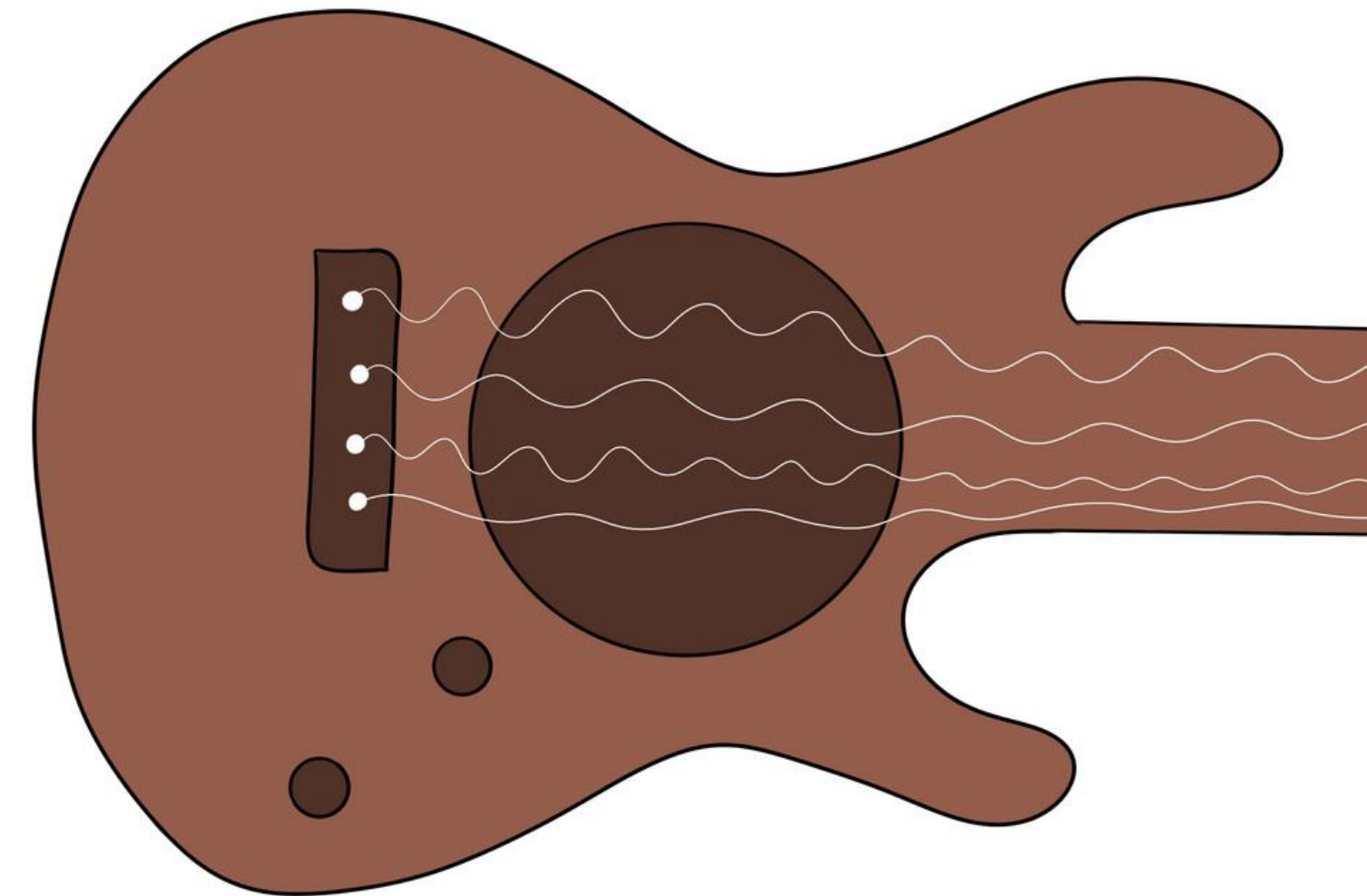
$$\frac{\partial^2 \psi}{\partial x^2} - \frac{1}{v^2} \frac{\partial^2 \psi}{\partial t^2} = 0,$$

where $v = \sqrt{T/\rho}$ while T is the tension force, and ρ is the linear mass density.

The eigenfrequencies of the oscillations:

$$f_n = \frac{nv}{2l}$$

where n is an integer representing the harmonics of the oscillation.



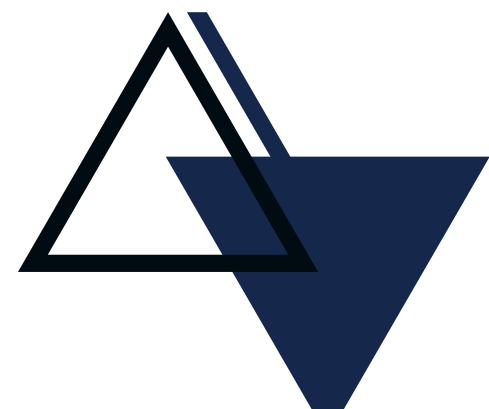


● Introduction



Few assumptions of the model:

- The ionosphere is a perfectly conductive layer where the two ends of the field-line are fastened (equinoxal model).
- The conductivity along the field lines approaches infinity.
- The perturbations along a field line do not perturb the nearby field lines.

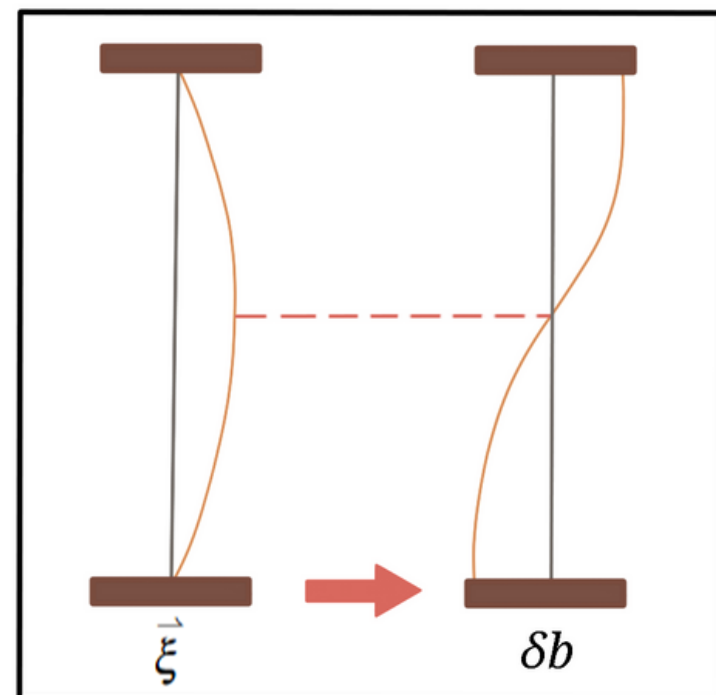


● Introduction

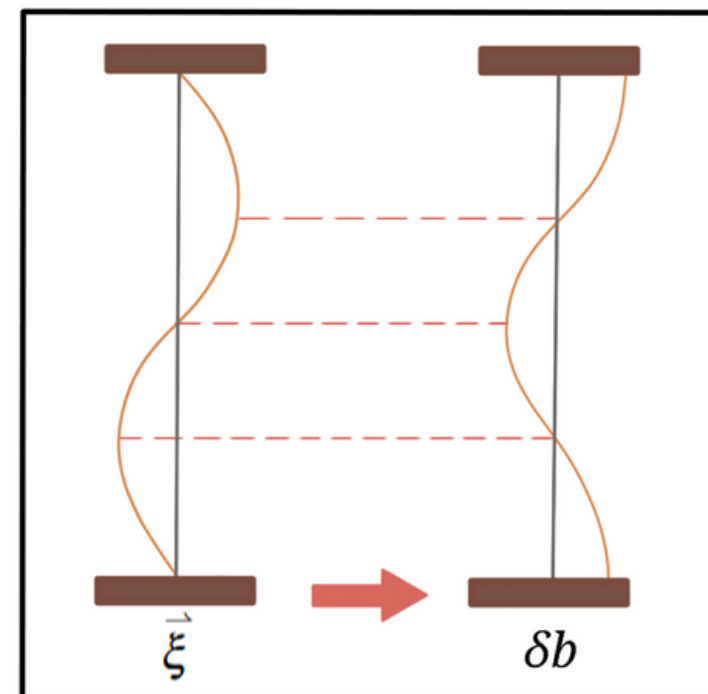
The electric and magnetic field perturbations using Ohms's law and Faraday's law can be proved to be:

$$\vec{E} = -\frac{\partial \vec{\xi}}{\partial t} \times \vec{B}_0 \quad , \quad \delta \vec{b} = B_0 \frac{\partial \vec{\xi}}{\partial s}$$

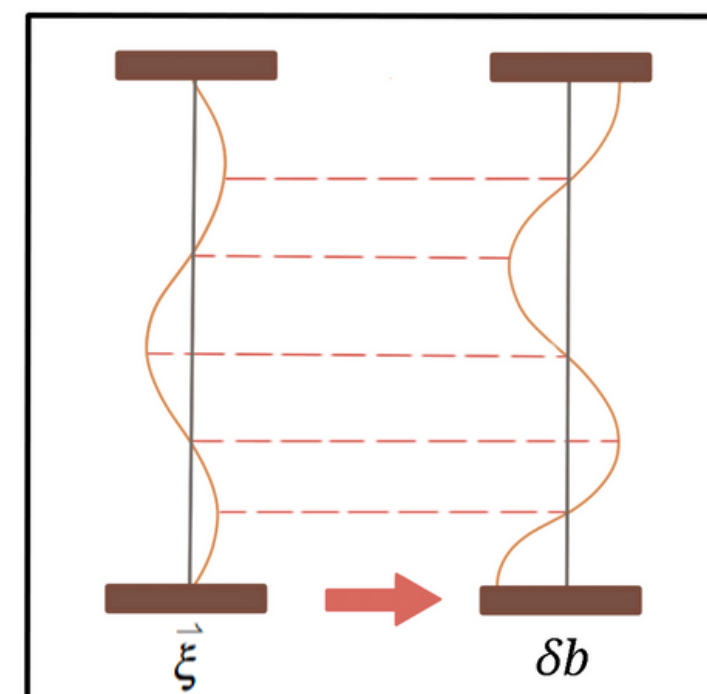
Fundamental Mode



Second Order Mode



Third Order Mode






● Introduction

The general wave equation of incompressible plasma for transverse wave modes becomes:

$$\frac{\partial^2 \vec{E}}{\partial t^2} - v_A \times v_A \times \vec{\nabla} \times \vec{\nabla} \times \vec{E} = 0$$

which is very complex to solve analytically.

Under perfectly transverse electric/magnetic field perturbations the solution decouples as toroidal or poloidal polarization modes with eigenfrequencies:

$$f_n = \frac{nv_A}{2l} = \frac{nB_0}{2l\sqrt{\mu_0\rho_m(r)}}$$


● Introduction

■ Poloidal mode:

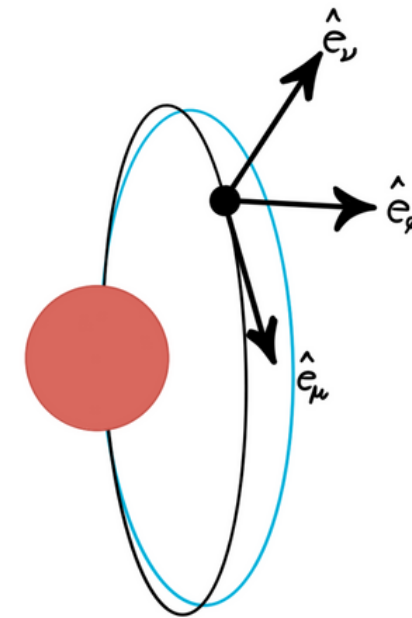
when the oscillation is mainly radial δb_v and E_ϕ ($k_\phi \rightarrow 0$).

■ Toroidal mode:

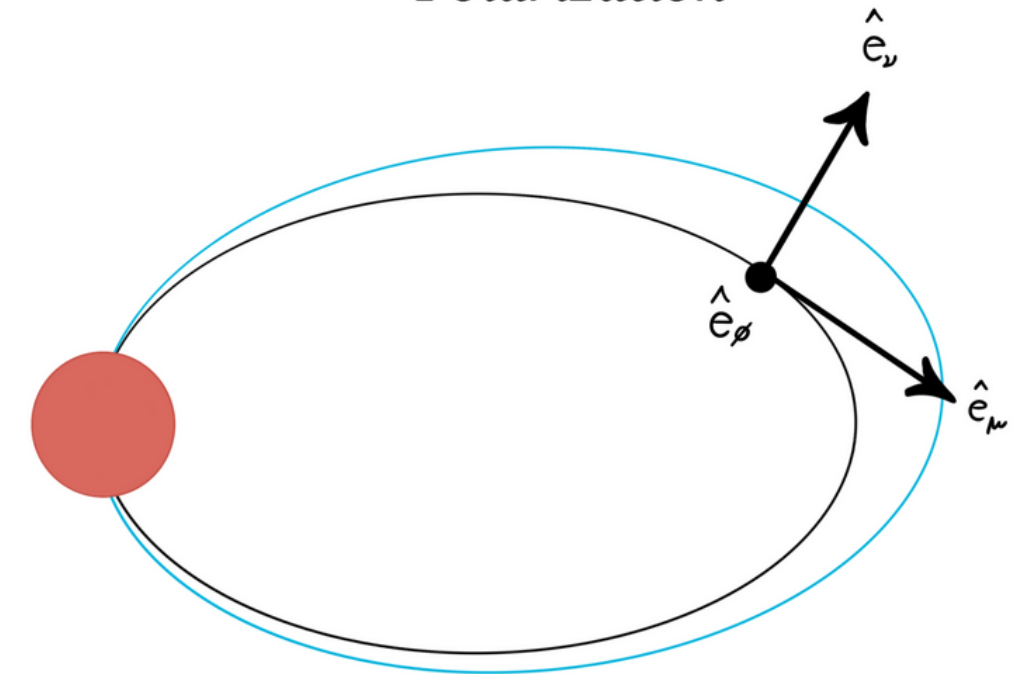
when the oscillation is mainly azimuthal δb_ϕ and E_v ($k_\phi \rightarrow \infty$).

These waves fall within the ultra-low frequency (ULF) range.

Toroidal Polarization




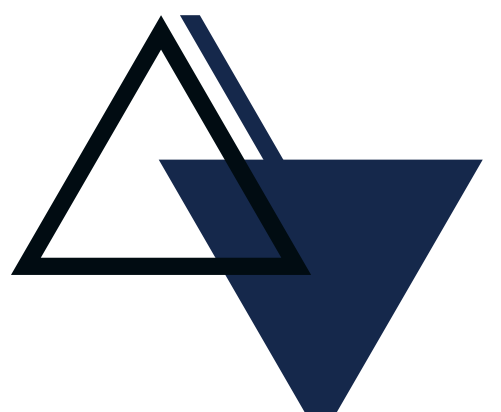
Poloidal Polarization

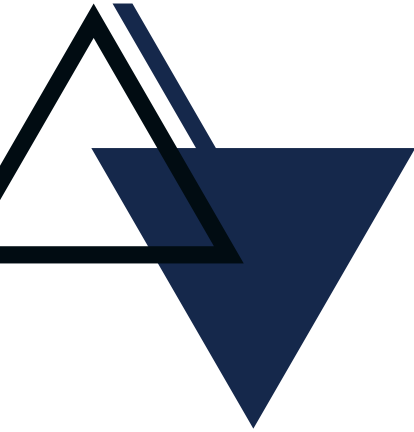




● Introduction

The magic resonant frequencies

- Earlier studies of ULF waves showed that there are seemingly preferred excitation frequencies of field-line resonances.
 - The first model used to explain the problem was the global cavity model.
 - Later in 2002 the solar wind dynamic pressure frequency astonishingly aligned with the ULF magic frequencies.
- 
- 



● Introduction



The Geomagnetic Pulsations

■ Geomagnetic pulsations:

The ULF variations (1 mHz – greater than 10 Hz) of the geomagnetic field.

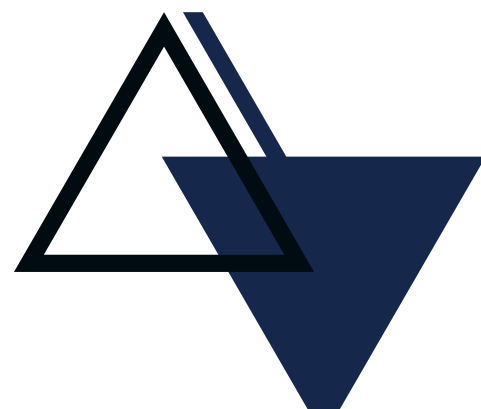
■ Continuous geomagnetic pulsations (Pcs):

The semi-sinusoidal continuous variations.

■ Irregular pulsations (Pis):

The irregular variations of the geomagnetic field.

Pulsations	T (s)	f	Amplitudes (nT)
Pc1	0.2–5	0.2–5 Hz	0.01–0.1
Pc2	5–10	0.1–0.2 Hz	0.1–1
Pc3	10–45	22–100 mHz	1–10
Pc4	45–150	7–22 mHz	5–50
Pc5	150–600	2–7 mHz	50–500
Pi1	1–40	0.025–1 Hz	0.2–1
Pi2	40–150	2–25 mHz	10–100





● Aim of Research

01

To highlight observational evidence of the influence of solar wind on geomagnetic events like the intense solar storm.

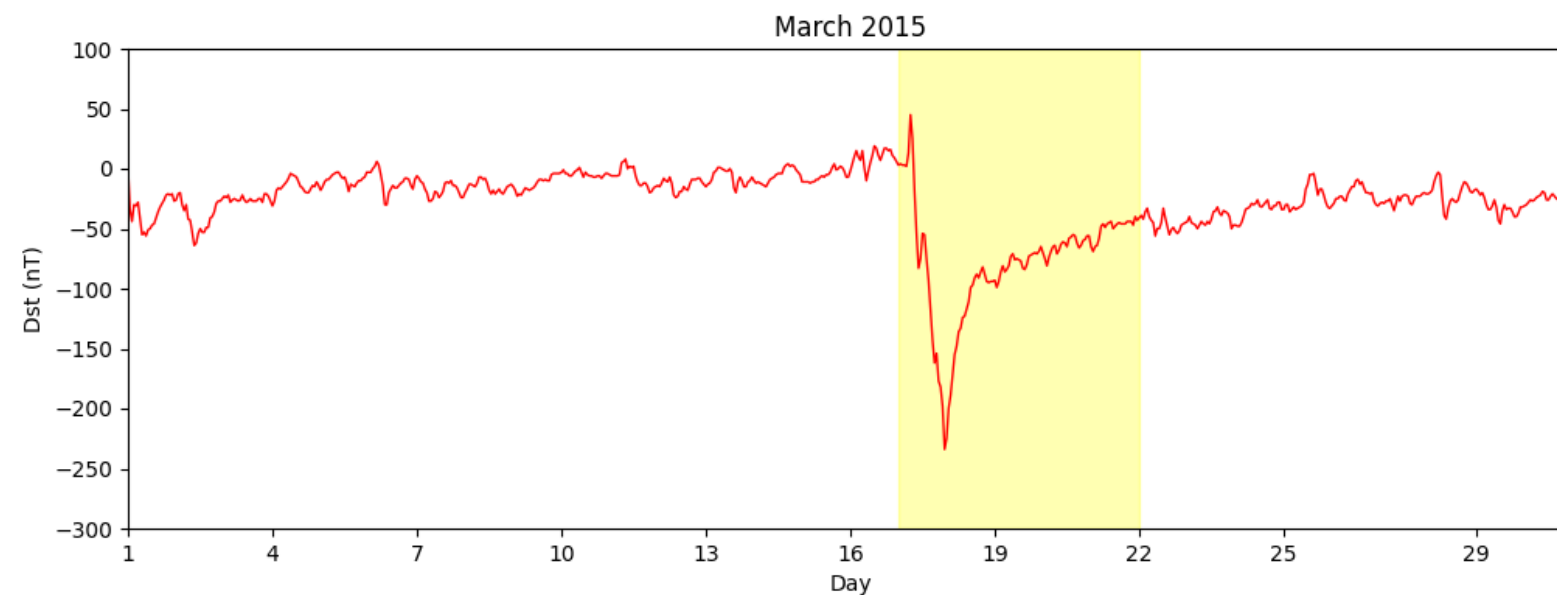
02

To study the overall distribution of Pcs and correlate them with the solar wind parameters in the equatorial region – as a potential method for distinguishing their sources–

● Methodology

Data Selection and Constraints

The 1 Hz data is taken from the global network of observatories INTERMAGNET of four longitudinally distributed stations selected to span the days 14–18 of March 2015 based on the Dst index records.



Station	Geomagnetic Latitude	Geomagnetic Longitude
GUAM (GUA)	5.76N	143.51W
DALAT (DLT)	2.19N	178.93W
ASCENSION Island (ASC)	2.73S	57.47E
KOUROU (KOU)	14.27N	20.46W



● Methodology

Data Selection and Constraints

Due to the Nyquist criteria, high-quality information can be obtained for the Pc3, Pc4, Pc5, and Pi2 pulsations only.

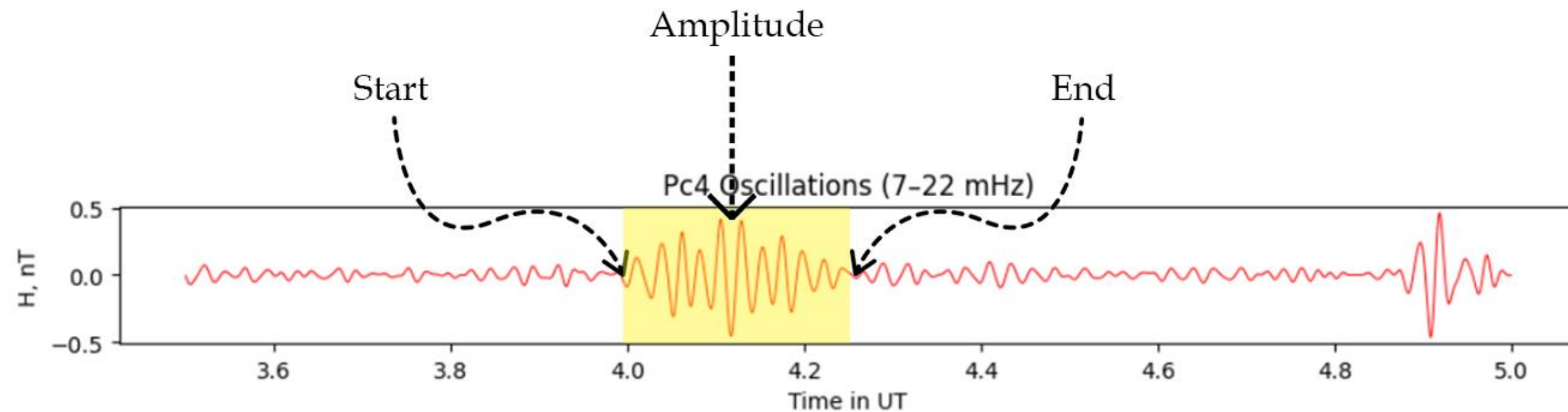
The solar wind parameters: IMF $|B|$, solar wind velocity, dynamic pressure, and the solar wind temperature of 1-minute resolution data time-shifted to the bow shock nose is taken from *omniweb*.



● Methodology

Data Selection and Constraints

- For pulsations distribution, a minimum of three cycles is required with thresholds: $Pc3 = 0.1 \text{ nT}$, $Pc4 = 0.3 \text{ nT}$, and $Pc5 = 0.5 \text{ nT}$.





● Methodology

Solar Wind Parameters Fitting

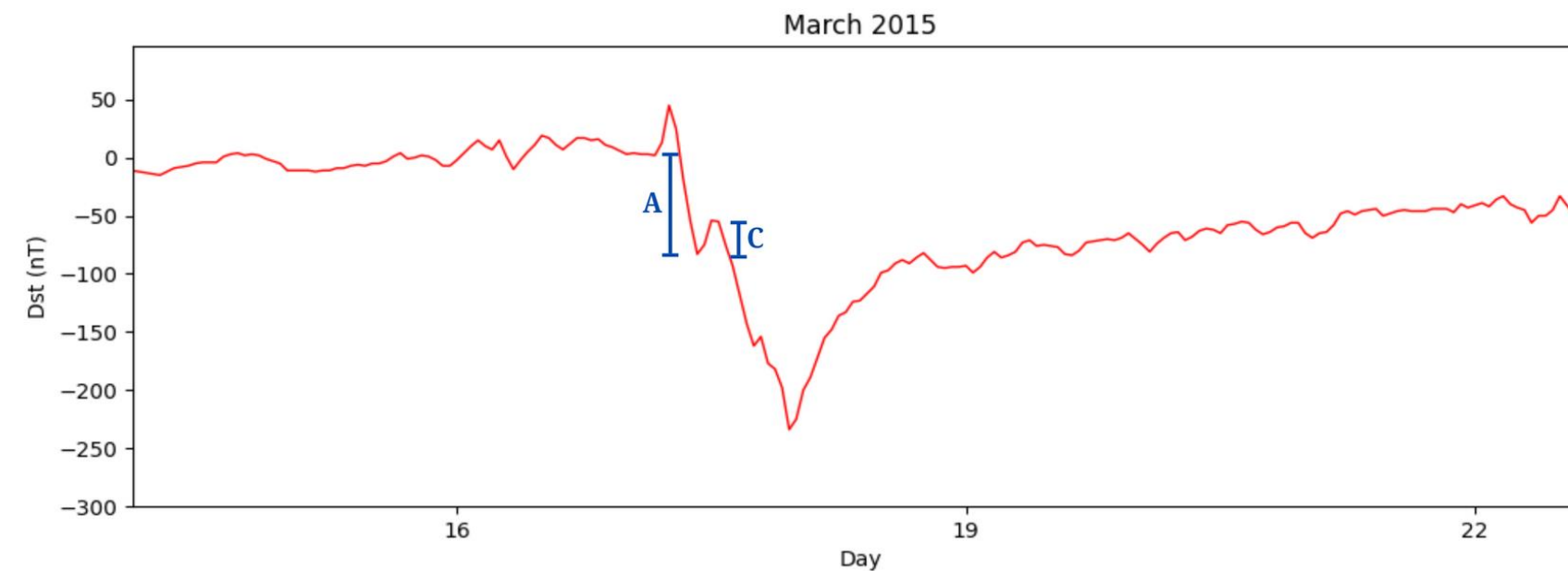
- To fit the solar wind parameters with the Pcs, the Welch method is applied on every 1-hour segment of ASC geomagnetic station.

$$\delta B = \sqrt{\int_{f_1}^{f_2} PSD_B(f) df}$$

where f1 and f2 are the minimum and maximum frequencies of each Pc type range.

● Results and Discussion

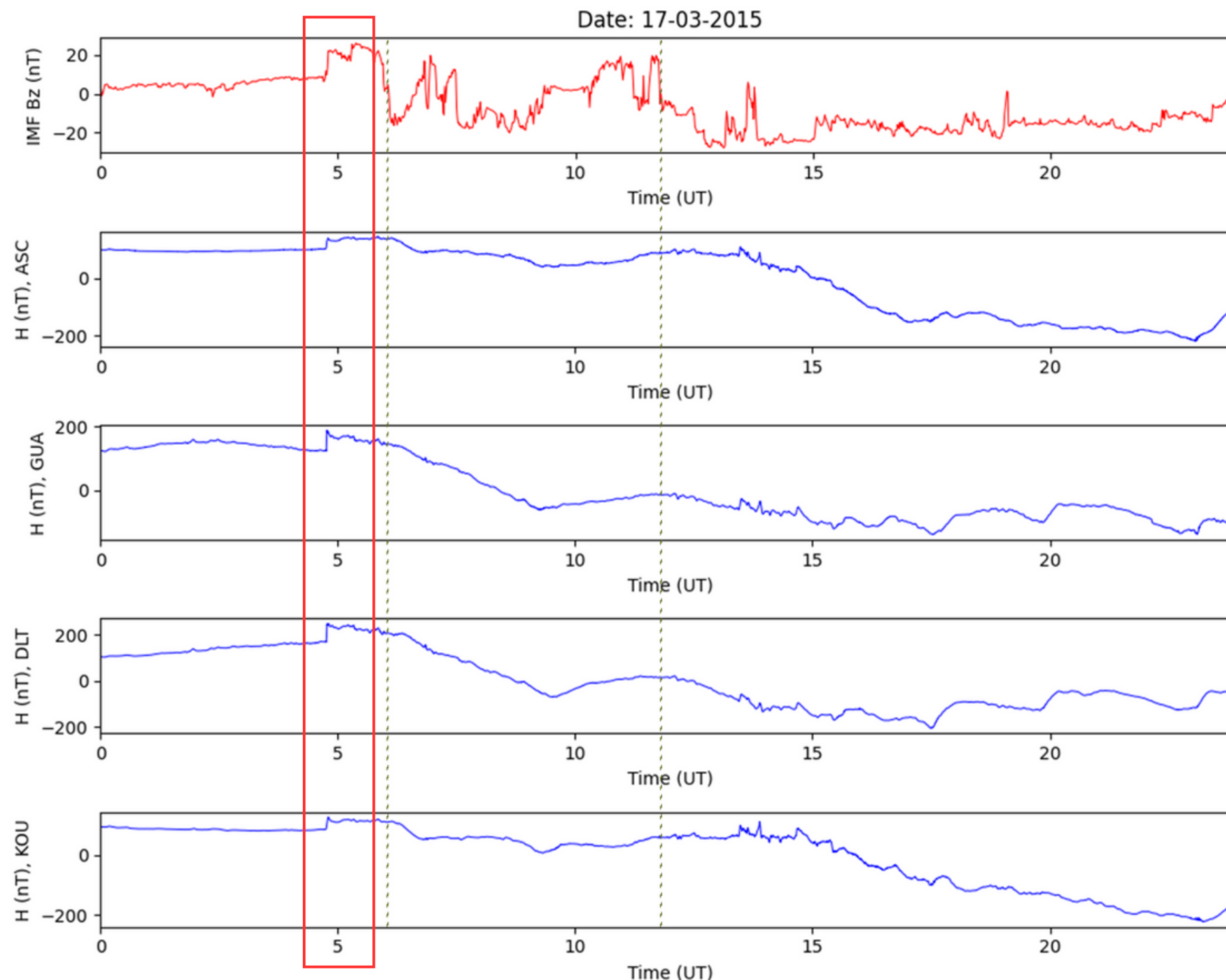
Features of March 2015 Solar Storm



- A minimum Dst of -234 nT.
- The SSC started on the 17th of March 2015 at around 4.8 UT.
- The main phase of the storm initiates around 6.0 UT and lasts up to 23.0 UT when the recovery phase starts and reaches an end on approximately the 22nd of March 2015.
- C/A factor is 0.414.

● Results and Discussion

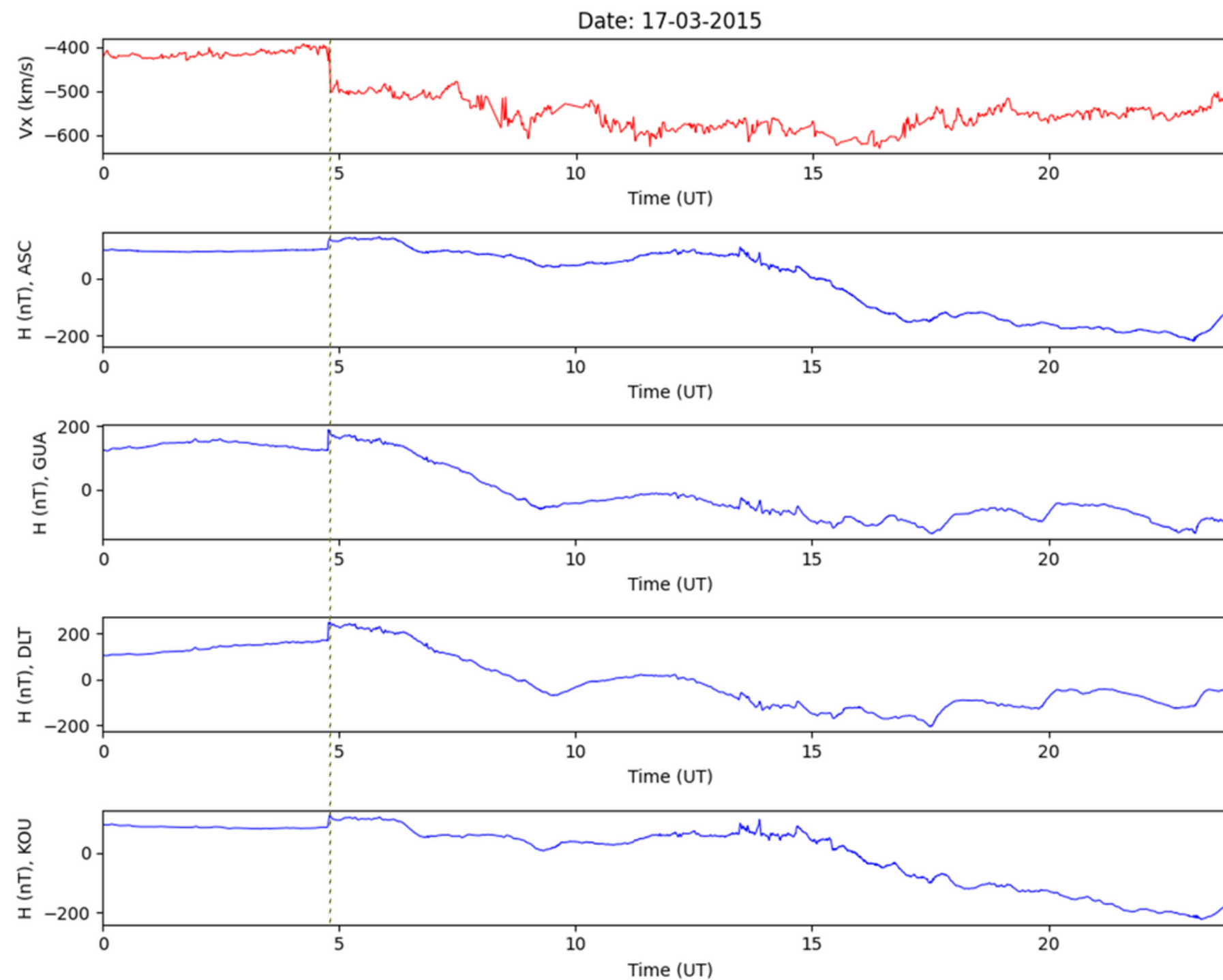
The Double Structure of the Storm Main Phase



- the IMF Bz data shows a double reversal of the Northward IMF Bz into a Southward IMF Bz at 6.1 UT and 11.8 UT respectively.
- the SSC also matches the arrival of higher amplitude IMF at around 4.8 UT.

● Results and Discussion

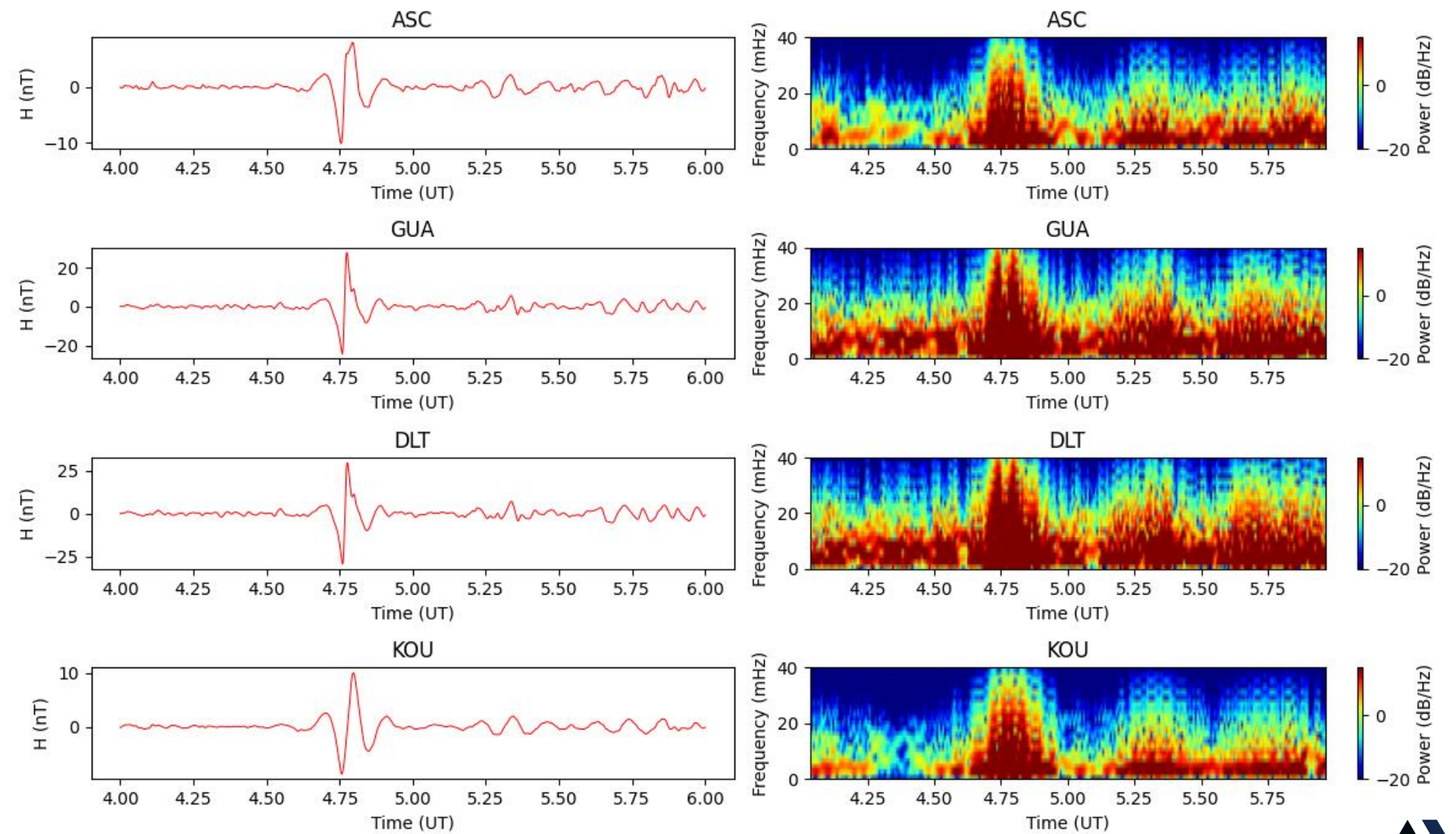
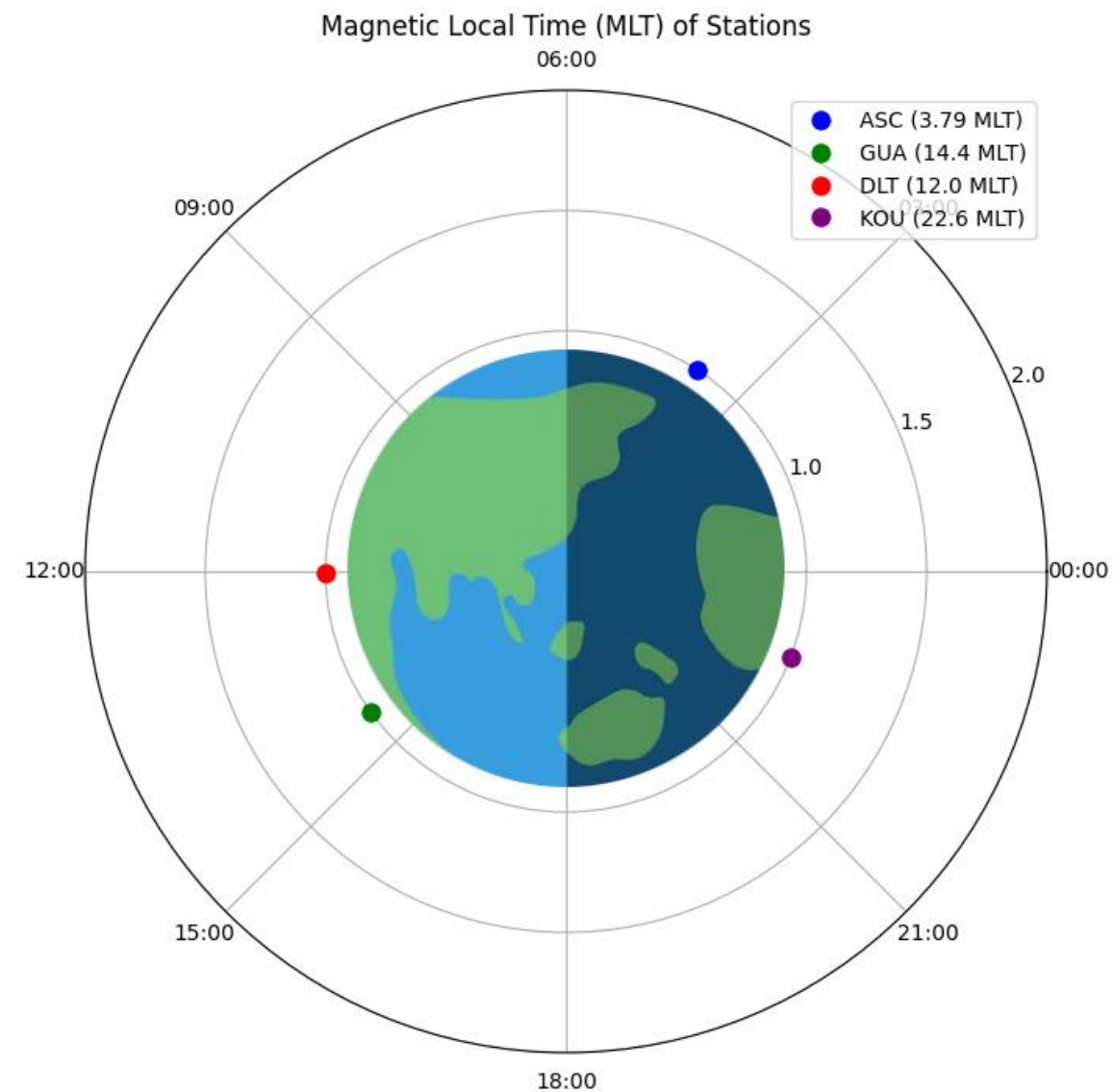
The SSC and the Upstream Solar Wind Speed



- The increase in the solar wind speed upstream of the bow shock in the dayside also is in sync with the enhancement of the H-component recorded by the geomagnetic stations.

● Results and Discussion

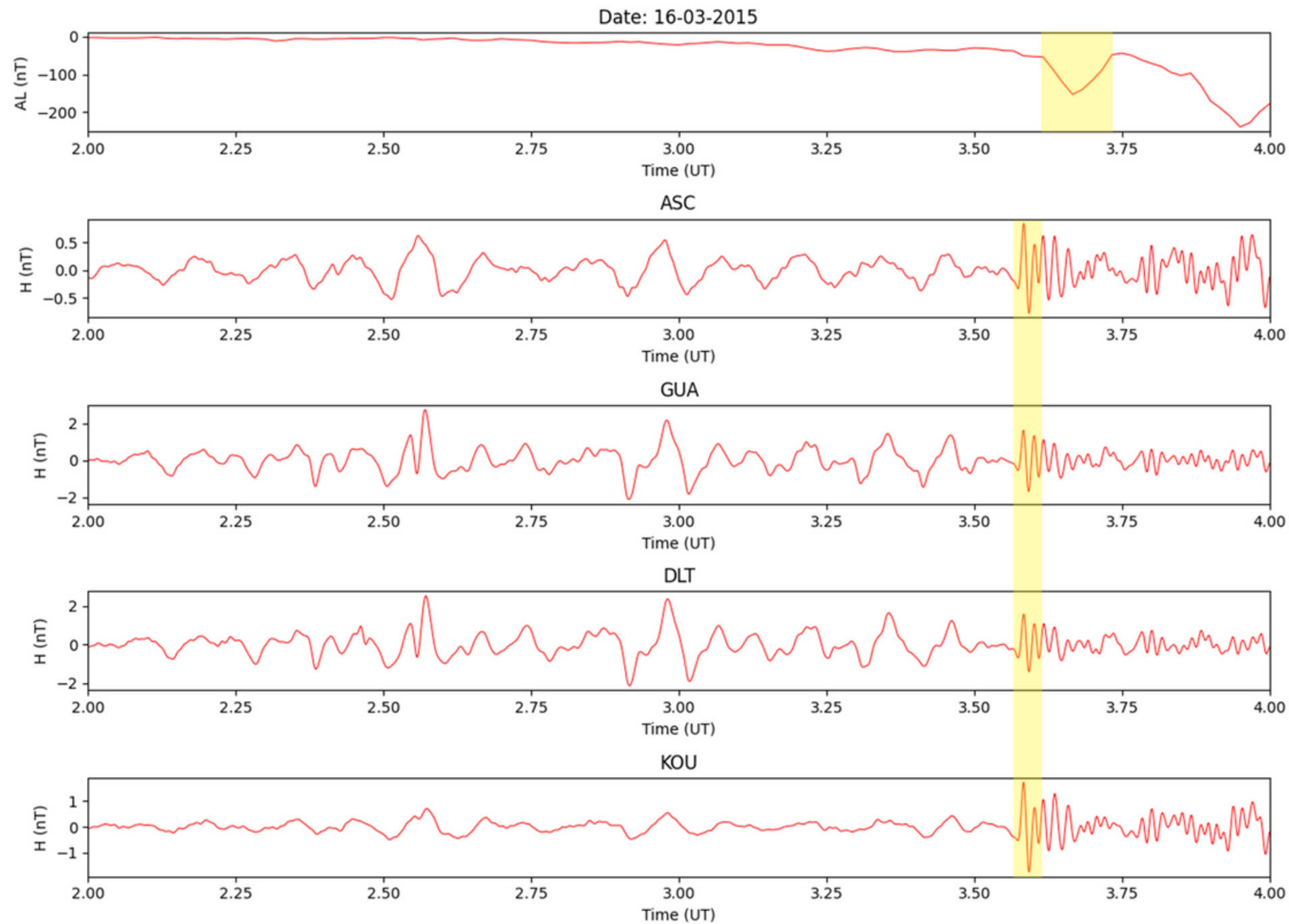
Pi2s Associated with SSC



- Peak-to-peak amplitudes: 18 nT for ASC, 52.0 nT for GUA, 59.5 nT for DLT, and 18.8 nT for KOU.

● Results and Discussion

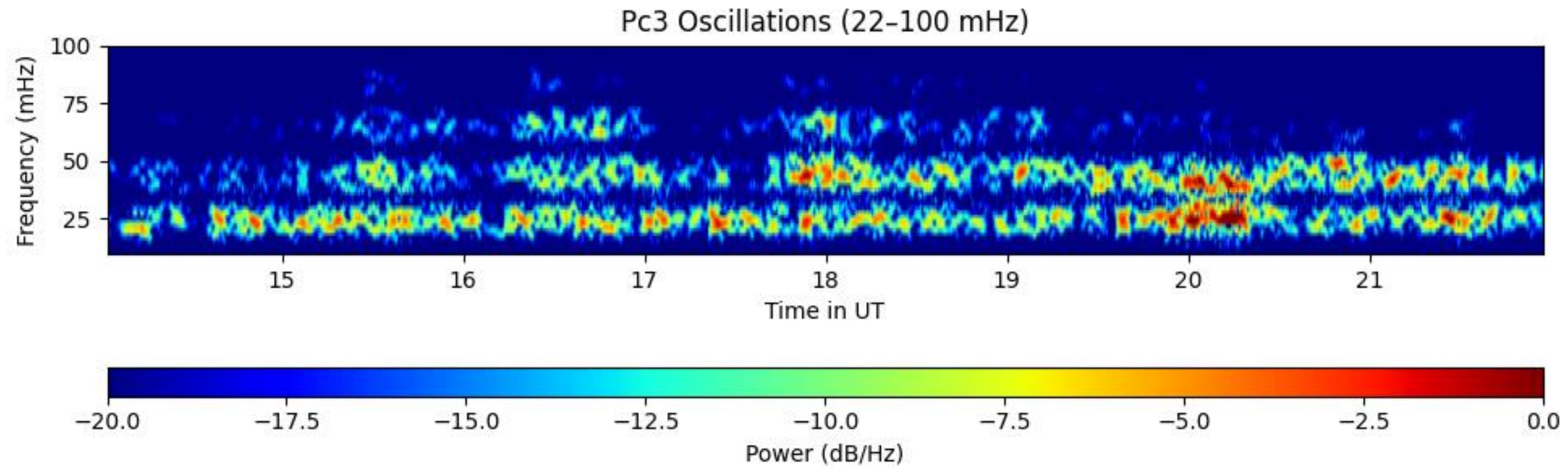
Pi2s as Substorms Precursor



- Pi2 events are also known to be precursors of geomagnetic substorms.
- Pi2 signal observed on the 16th of March at 3.6 UT exhibits a good concordance with the AL index.
- The auroral currents take some time to develop and induce a magnetic field in the auroral region.

● Results and Discussion

Field Line Resonance Signature

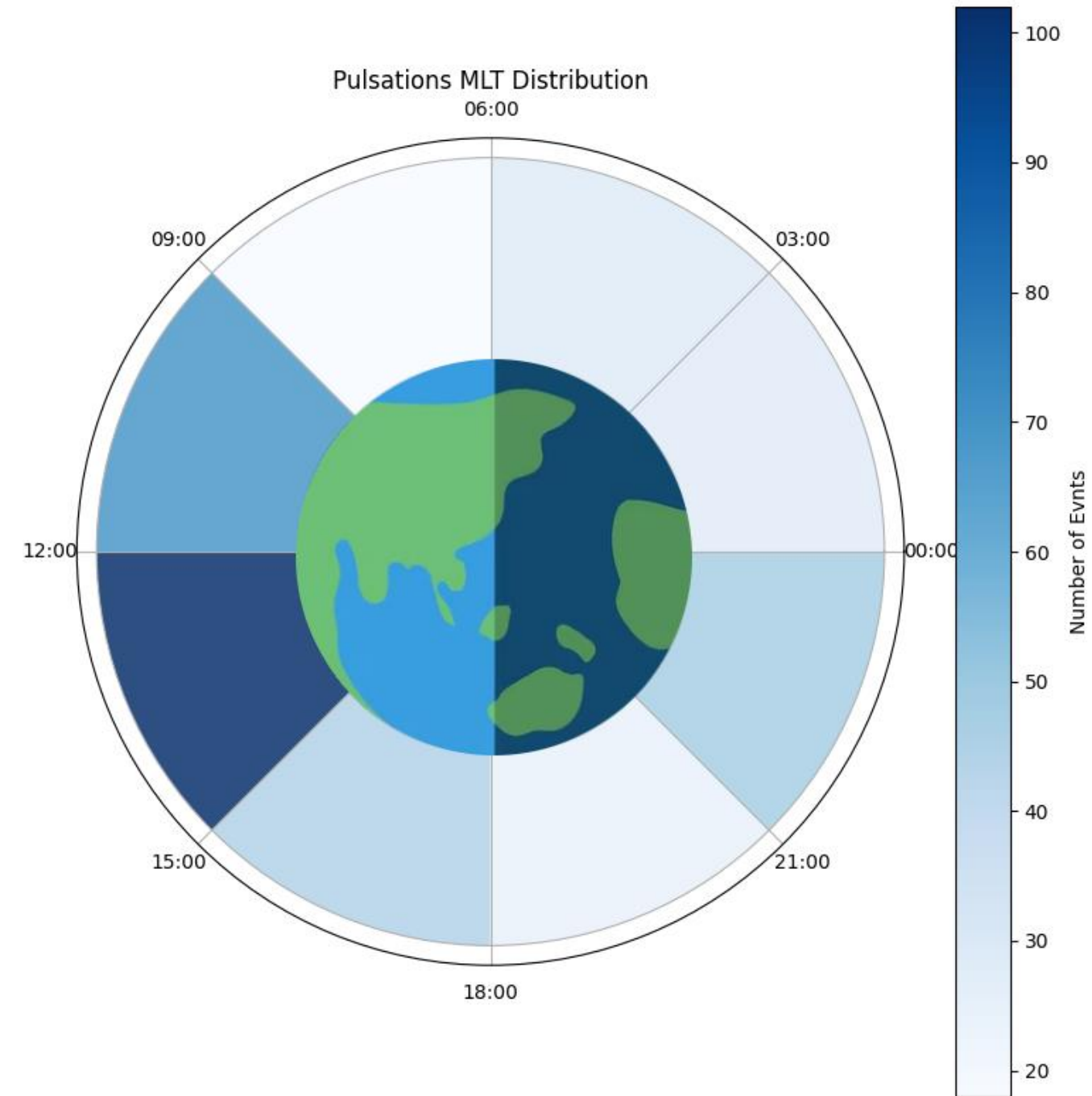


- At the ASC station on the 16th April shows astonishingly clear field-line resonance feature.
- The power of the pulsations at each of the resonance frequencies decreases for higher harmonics as expected.

● Results and Discussion

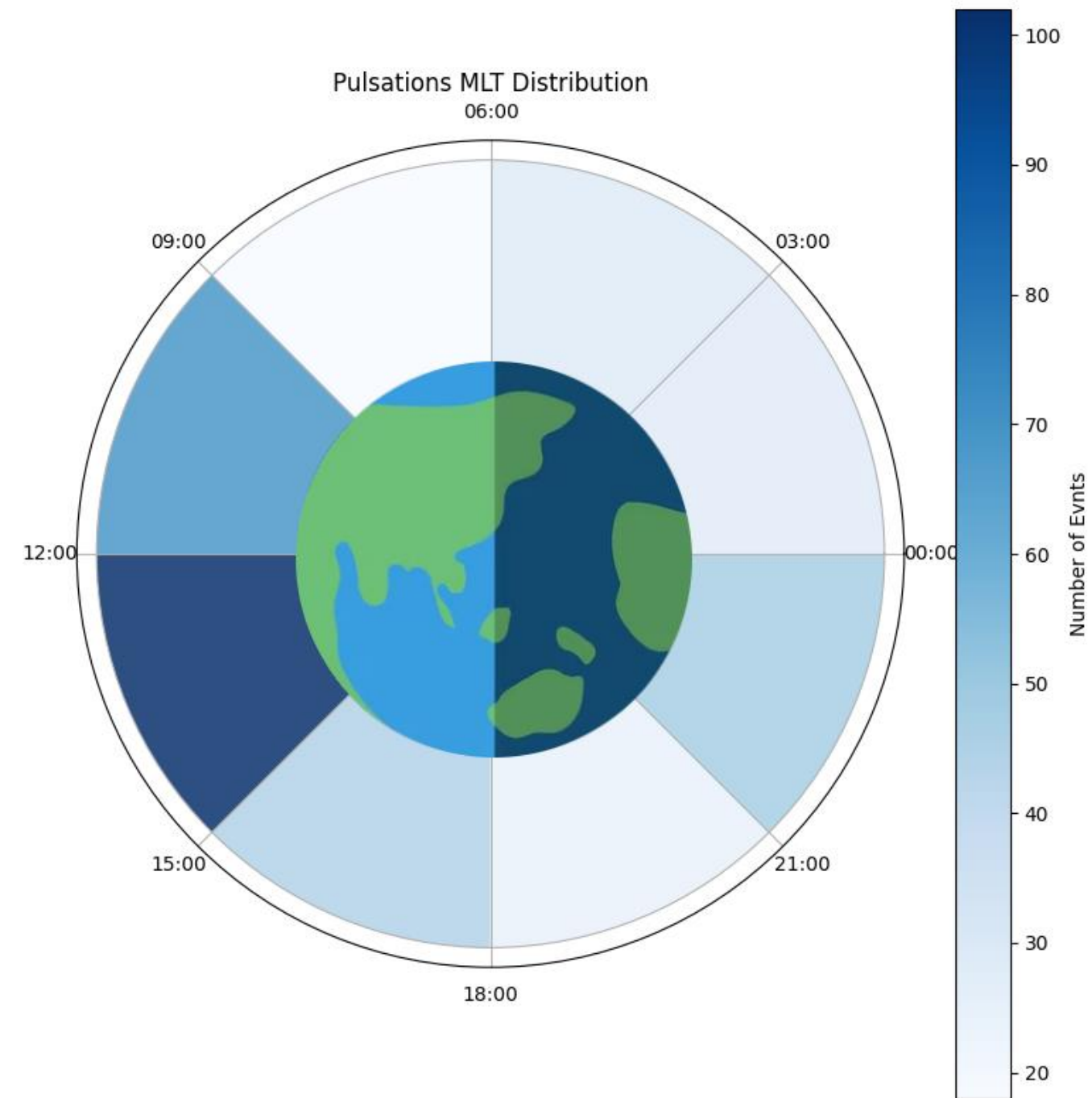
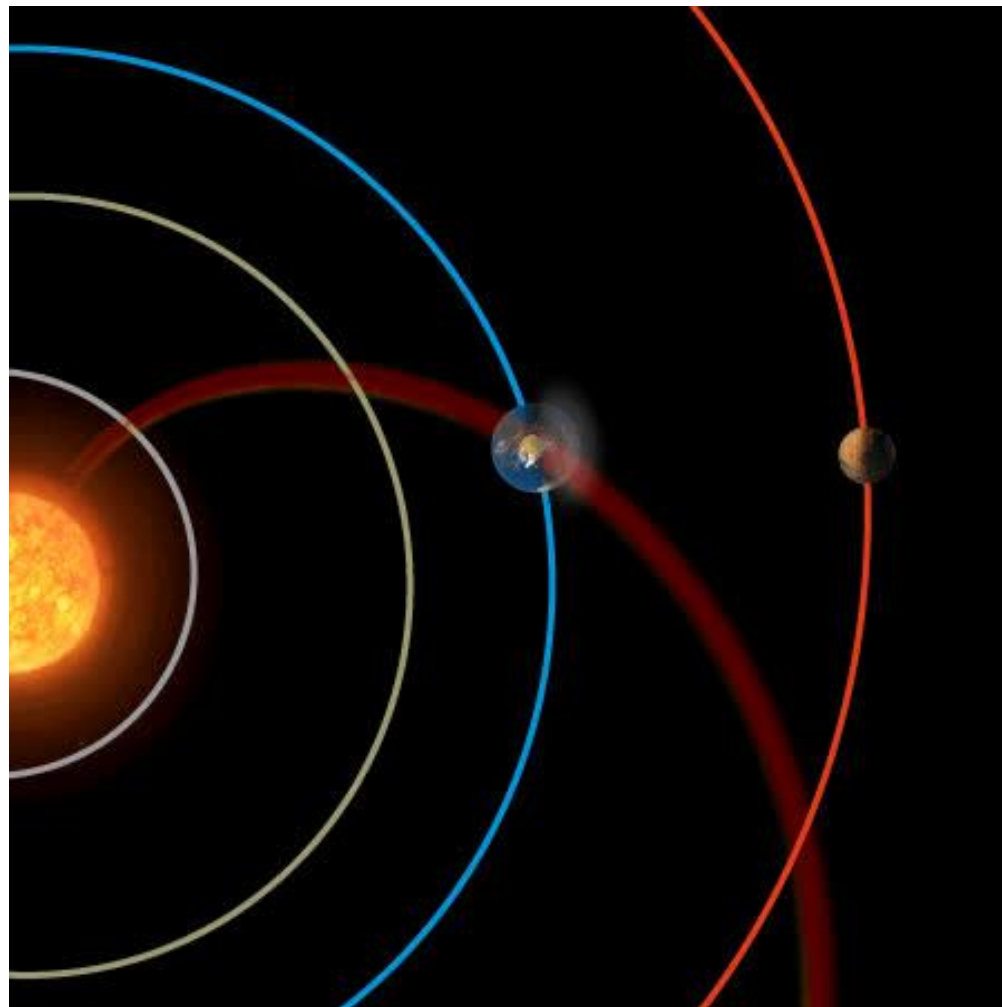
MLT Distribution of Pulsations

- The recorded pulsations seem to have dayside bow-shock preference suggesting that the ULF pulsations in this analysis are directly generated from the solar wind time-varying compressions.



● Results and Discussion

MLT Distribution of Pulsations

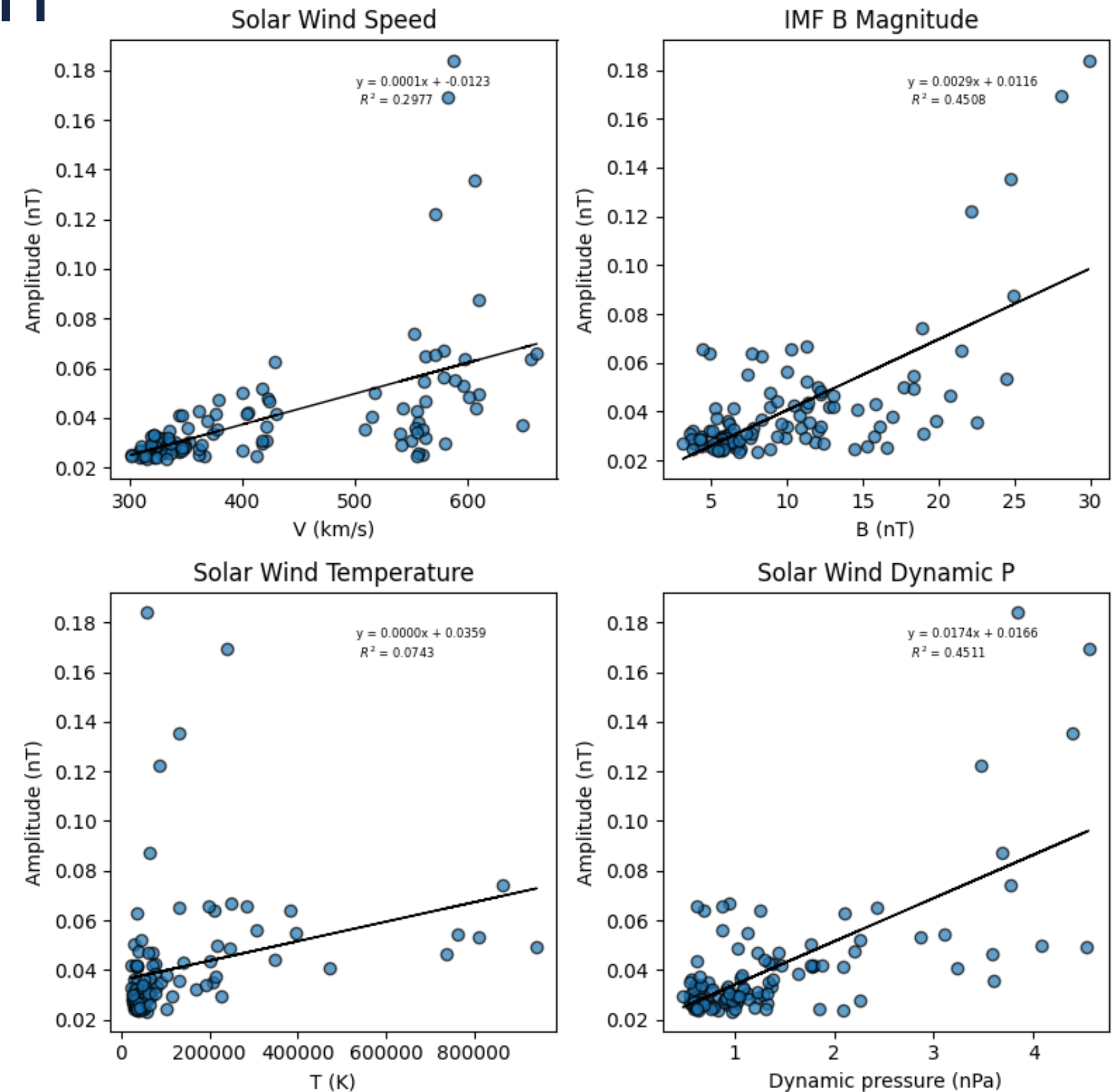


- It shows a strong agreement with the expected arrival of the solar wind.

● Results and Discussion

Parameters Analysis

- The SW speed, IMF B magnitude, and SW P have an average R^2 values of 0.2099, 0.4491, 0.4318 respectively.
- The SW T exhibited a minimal association with $R^2 = 0.0743$ for Pc3, $R^2 = 0.0814$ for Pc4, and $R^2 = 0.1218$ for Pc5.
- The overall parameters do not show significant distinction between Pcs.





Conclusion

- ULF pulsations are very important to diagnose the overall geomagnetic field.
- Analysis of the solar wind IMF Bz and Vx variation showed a great concordance with March 2015 solar storm features.
- Pi2 association with impulsive source as well as being precursors of substorms was identified.
- A resonance of the field-line feature in ASC geomagnetic station was detected.
- The distribution of Pcs exhibited a subsolar bow shock preference.
- Pc3–Pc5 pulsations amplitudes showed a good relationship with the SW speed, IMF B, SW P, but a minimal correlation with the SW temperature with no distinction among the Pcs.



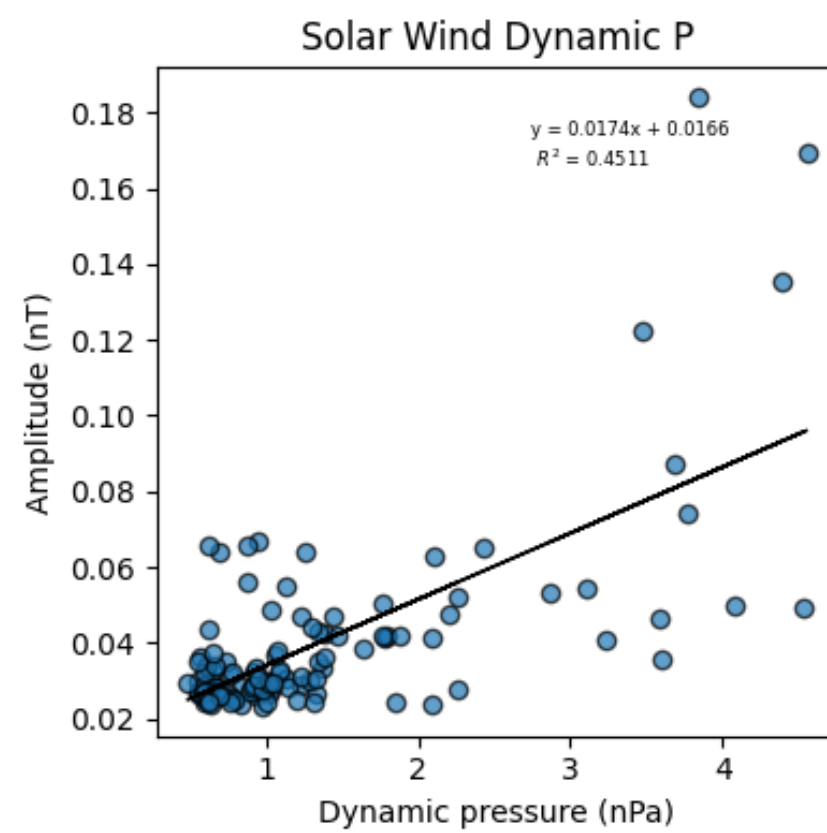
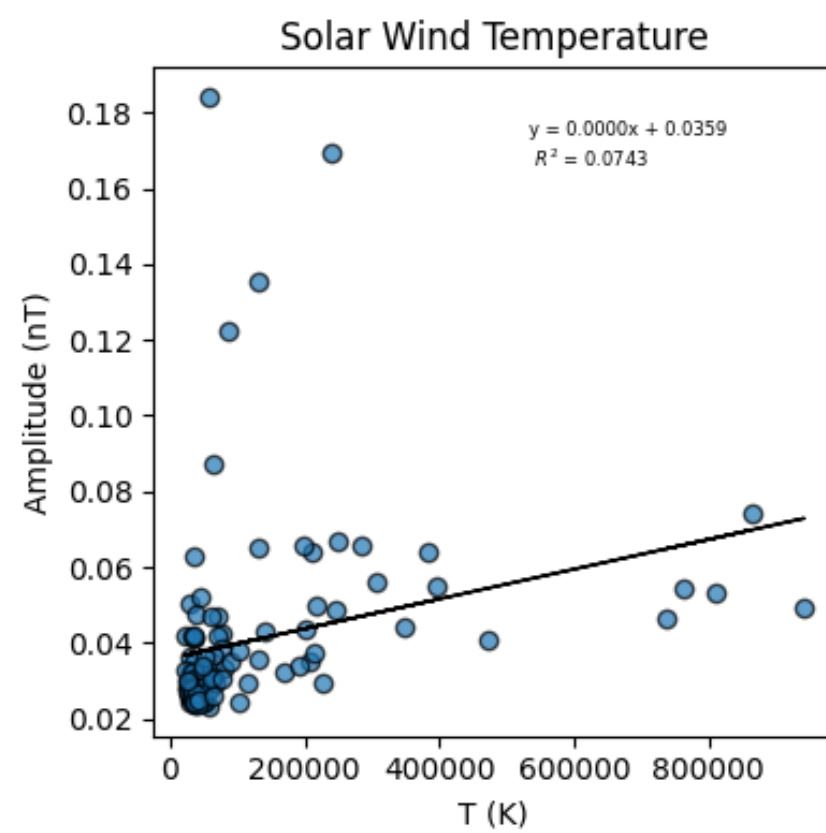
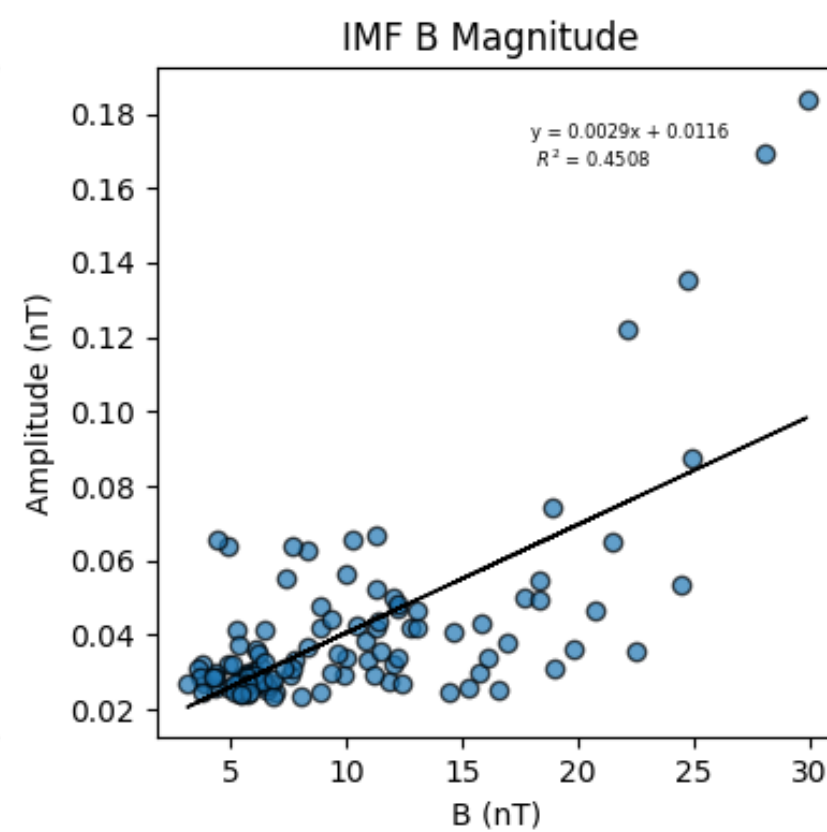
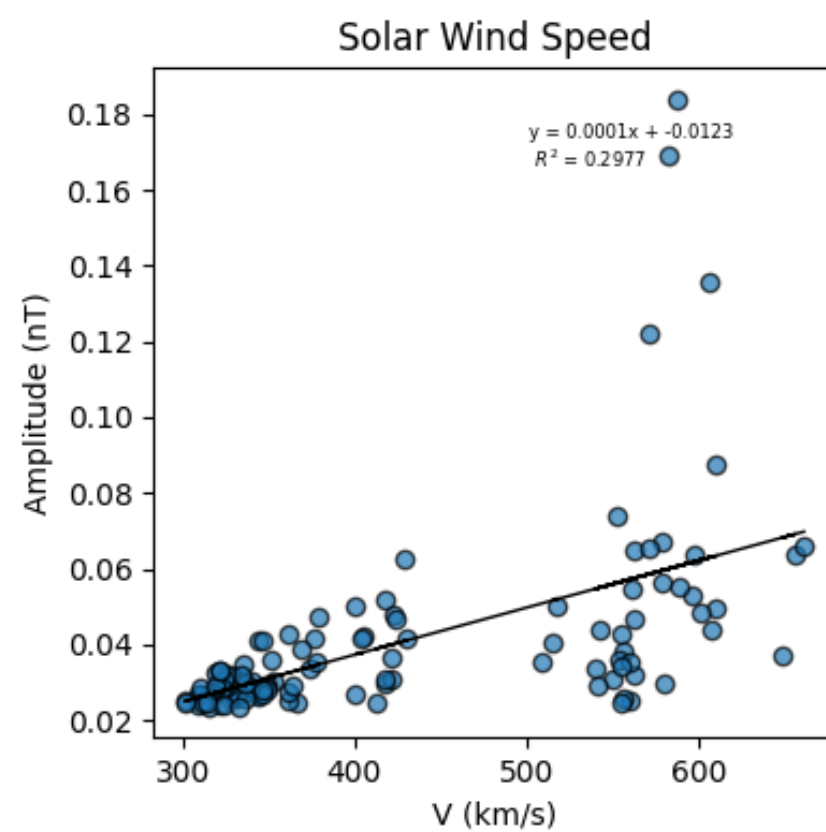
Future Work

- Further investigations involving the cone angle ($\theta = \cos^{-1} B_x/|B|$) is required to confirm that the source of pulsations in this study are upstream compressional waves.
- To examine the solar cycle dependence of the distribution of pulsations in MLT.
- Considering other methods of computing the MLT of pulsations.
- A better analysis could be achieved using satellite in-situ data, as the amplitudes of pulsations significantly reduce as they reach the ground station.
- Incorporating latitudinally distributed stations data.
- Using machine learning to automate events selection procedure.

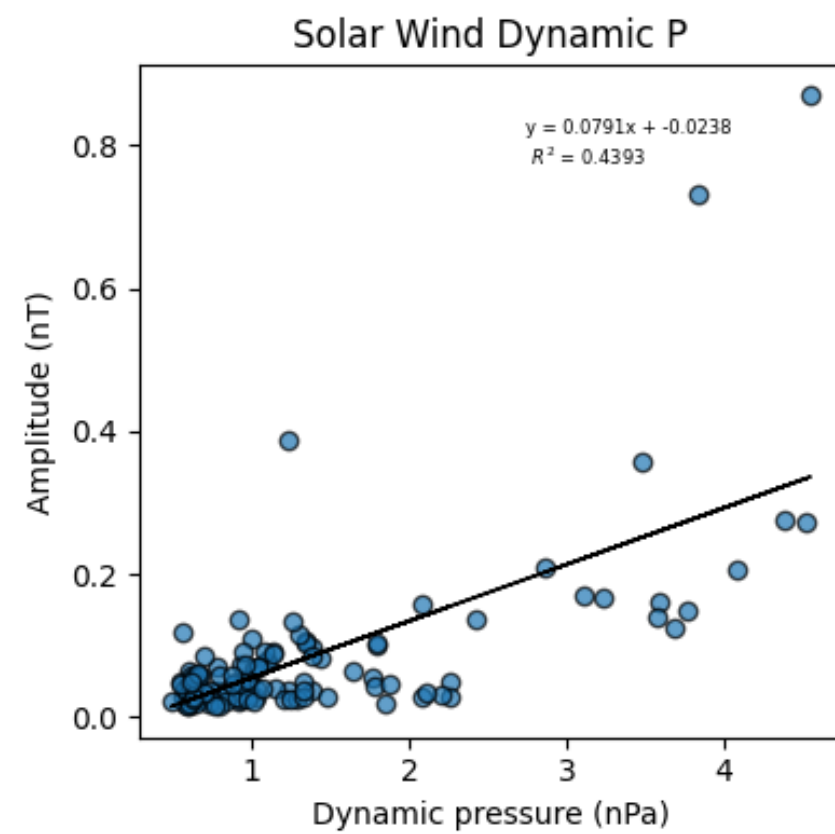
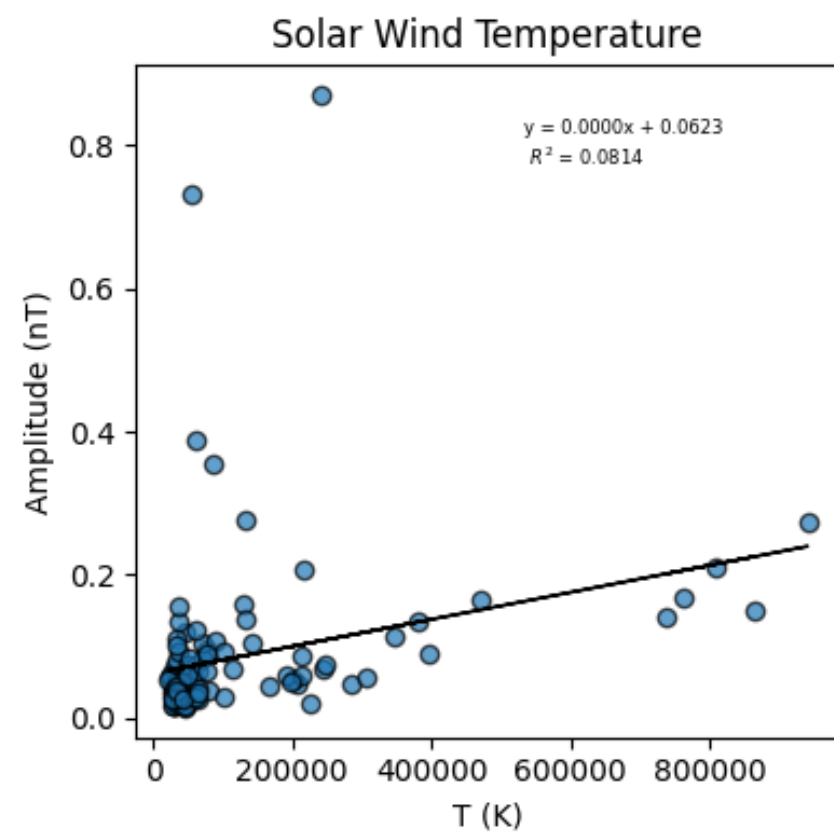
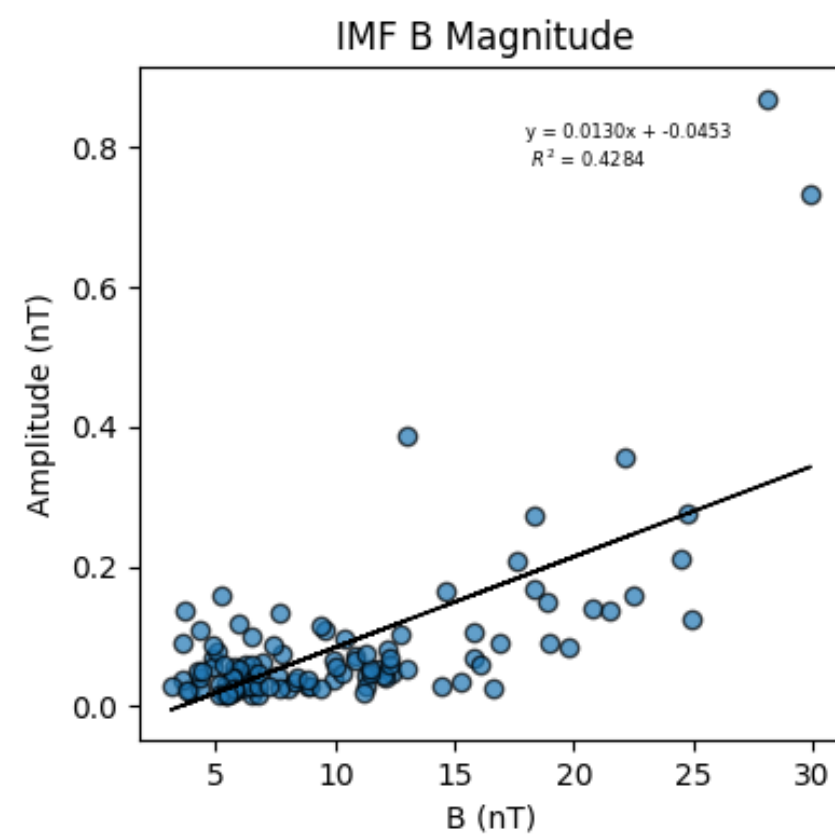
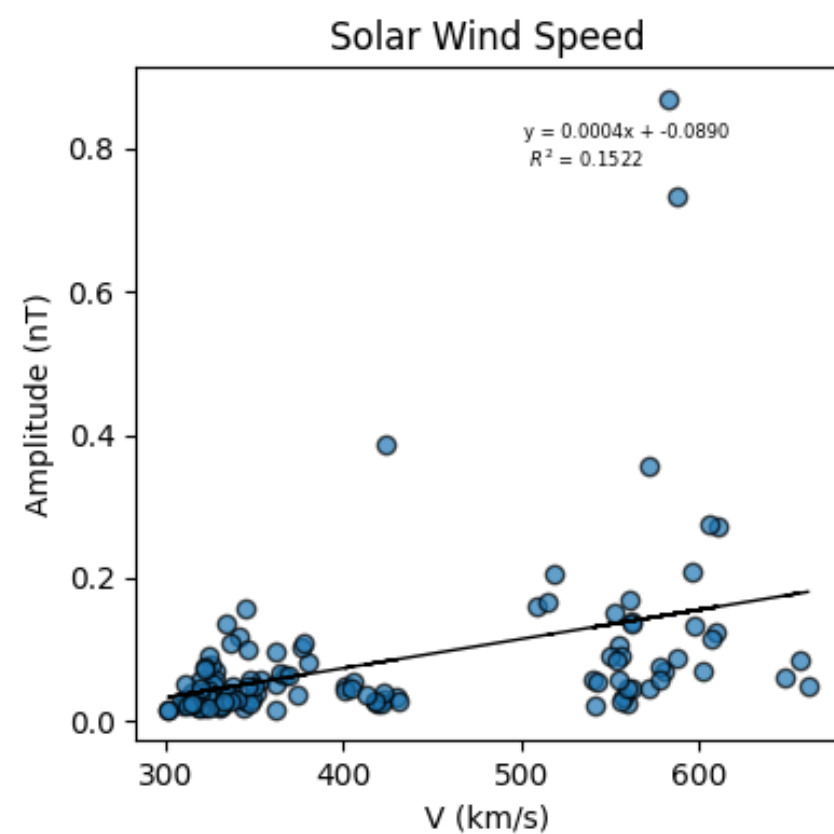


THANK YOU!

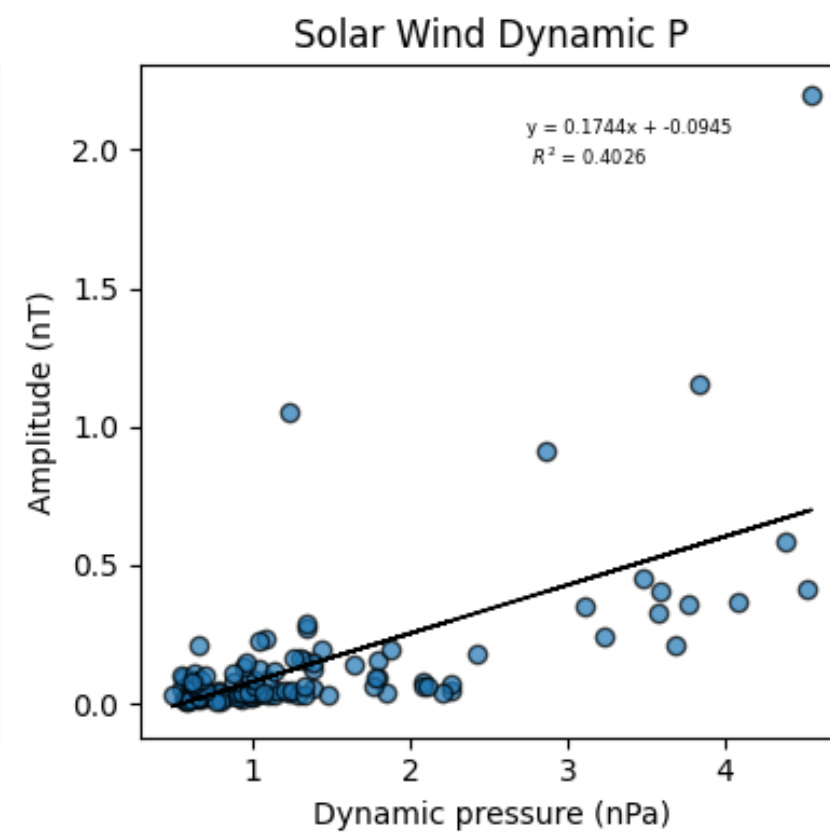
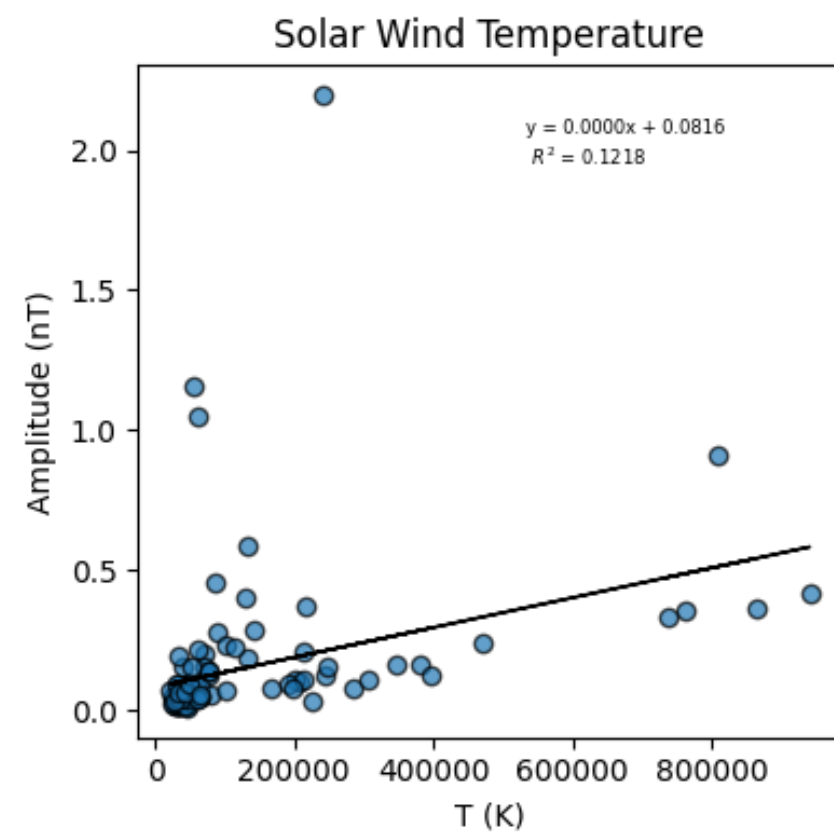
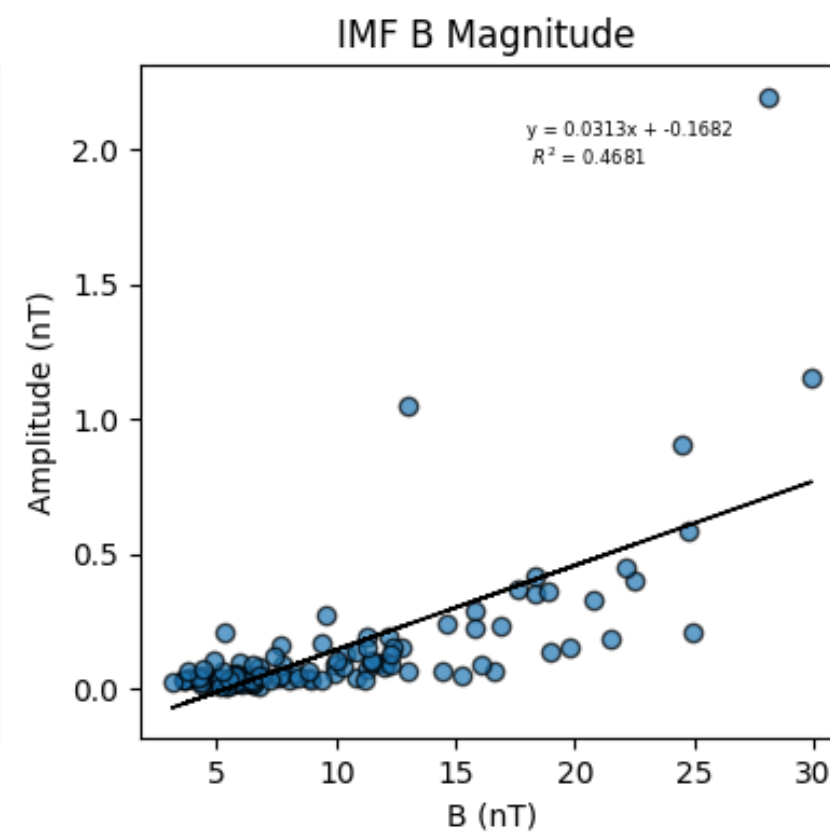
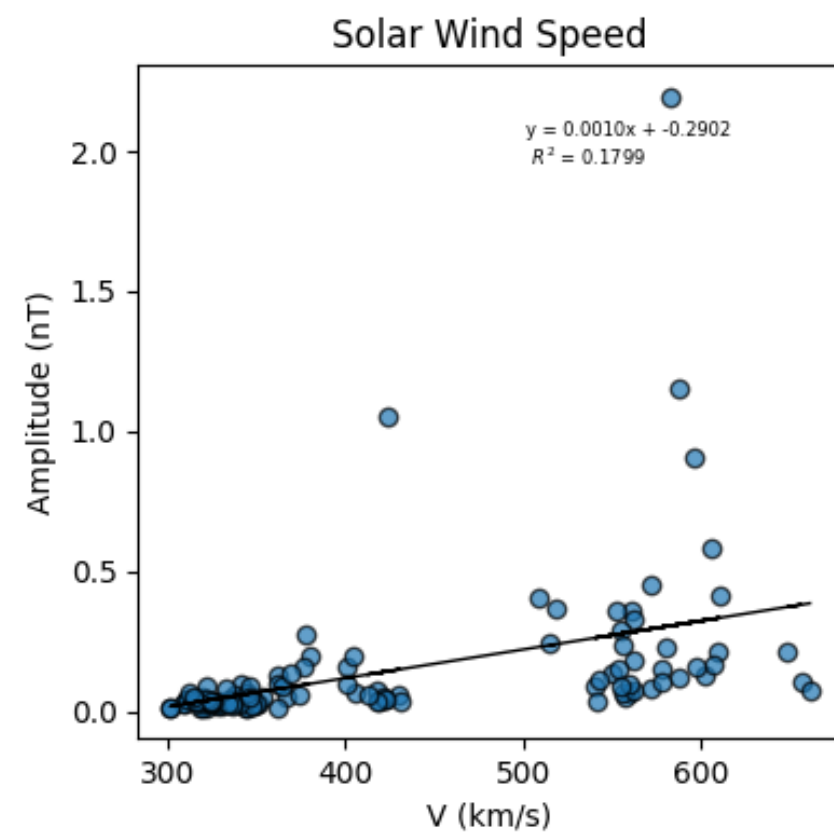




Pc3



Pc4



Pc5

● Introduction

- 'Quebec Interconnection' had a 9 hours blackout on March 1989 intense storm.
- Geomagnetically induced currents damaged the transmission lines of Quebec Interconnection.
- Deficiencies in the power plants extended to the United States, United Kingdom, and Sweden.

